SiliconPV 2023, 13th International Conference on Crystalline Silicon Photovoltaics
Carrier Selective Contacts, Metallization and Contact Formation
https://doi.org/10.52825/siliconpv.v1i.884

Published: 29 Feb. 2024

Tailoring of Interface Quality of MoO_x/Si Solar Cells

Abhishek Kumar[1, 2] [https://orcid.org/0009-0004-5571-4120], Jyoti[1, 2], Shweta Tomer[1, 2], Vandana[1, 3], S. K. Srivastava[1, 2], Mrinal Dutta[4] and Prathap Pathi[1, 2]

[1] Academy of Scientific and Innovative Research, India

[2] CSIR - National Physical Laboratory, India

[3] CSIR – AMPRI, India

[4] National Institute of Solar Energy, India

Abstract. Transition metal oxide films (TMO) as passivating contacts with improved opto-electronic characteristics play an important role in improving the silicon solar cell device efficiency. In this report, the effect of sputtering power on the optical properties of MoO_x and the quality of MoO_x/n-Si interface for its application in a silicon solar cell as carrier selective contacts has been reported. The optical transmittance of the film greater than 80 % in the visible and near infrared region of the spectrum is observed, which further improved with sputtering power. The formation of oxygen ion vacancies, which operate as positively charged structural defects capable of capturing one or two electrons, caused the optical band gap to narrow from 3.70 eV to 3.23 eV at higher power. The oxygen vacancies occupied by electrons, which operate as donor centers close to the valence band, were responsible for electrical property modulation. The electrical properties of MoO_x/n-Si interface was analyzed using current-voltage (I-V) measurements for its application as selective contact. A significant change in the selectivity parameters, like barrier height, I_0 and series resistance of MoO_x, has been observed with dc power. These extracted parameters showed that the sputtering power has a great influence on the selectivity of the charge carriers.

Keywords: Transition Metal Oxides, Selective Contacts, Sputtering, Barrier Height.

1. Introduction

The transition metal oxides (TMOs) have found vast applications within the domain of electronic and optoelectronic devices, such as solar cells, photodetectors, and light-emitting diodes [1, 2, 3, 4]. TMOs have the ability to change their optical absorption properties on light irradiation, heat absorption and application of external electric field, i.e., why they are also popular as chromogenic materials. TMO ultrathin films have demonstrated the feasibility of miniaturizing electrical and optoelectronic devices. Among the TMOs, molybdenum oxide is very interesting in this regard, since they show a wide range of stoichiometric structures with different and enhanced properties according to its application [5]. MoO_x has been discovered to have fascinating uses in industry, such as high-density memory and electrochromic devices [6]. They're also widely utilized in energy storage and conversion, catalysis, transistors, and photovoltaics. Thermal evaporation [7], sputtering [8,9], chemical vapor deposition (CVD) [10], electrode deposition, and flash evaporation [11] are currently employed for MoO_x thin film deposition. Reactive sputtering is an excellent technique for modifying a wide range of optical and electrical properties of transition metal oxides and can be tuned by controlling the plasma density, oxygen partial pressure, and deposition pressure during the sputtering process. One of the main advantages of sputtering is control on growth of MoO_x of desired thickness and dep-

osition on large area with good stoichiometry. MoO_x exhibits a variety of stoichiometric structures from MoO_2 to MoO_3 with various phases in between such as Mo_4O_{11}, $Mo_{17}O_{47}$, Mo_5O_{14}, Mo_8O_{23}, etc. Till date, very few investigations have been reported on the room temperature grown as-deposited amorphous molybdenum oxide thin films with dc reactive sputtering of Mo target in O_2 and Ar ambient. The influence of deposition parameters on the rectification behavior of MoO_x on silicon has not been explained in details in the literature. In this study, we are reporting the tuning in the optoelectronic properties of as-deposited MoO_x thin films with variation in dc reactive power during the growth process. The presence of stoichiometric MoO_x plays a crucial role in the selectivity of charge carriers when this is used as carrier selective contacts in heterostructure silicon solar cells [12]. Also, the barrier height at the silicon interface influences the selectivity performance of the device. So, here we have presented the tailoring of rectification behavior of the device with dc power. The selectivity of the device is generally affected by the barrier height, J_0 and the contact resistance [13]. So, in order to use MoO_x as selective contact, higher barrier height and minimum J_0 and series resistance are basic requirements.

2. Experimental Details

The fabrication of MoO_x based Al/MoO_x/c-Si heterostructures were realized by DC reactive sputtering of Mo target in Ar+O_2 ambient on 1-3 Ω.cm n-type (100) FZ c-Si wafers and glass substrates. The wafers were cleaned by standard RCA1 and RCA2 cleaning procedures and afterwards, they were dipped in a dilute hydrofluoric acid (HF) solution (~10%), rinsed in deionized water and dried. Prior to the deposition, the sputtering chamber was initially cleaned and evacuated to a base vacuum of 1.5 $x10^{-5}$ mbar and the flow of gases in the sputtering chamber was managed by mass flow controllers (MFCs) during deposition. Pre-sputtering for 10 minutes was performed before depositing the film on each substrate to ensure the same condition by removing the oxide layer. The MoO_x layers were deposited at a deposition pressure of 7 $x10^{-3}$ mbar on one side of the c-Si wafers, for 20 minutes. The thickness of deposited film was measured by spectroscopic ellipsometry. Upon completing the rear side HF treatment process, full-area aluminum (Al) was thermally evaporated on c-Si substrates, with the thickness of ~500 nm. For all deposition schemes, the thermal evaporation system was vacuumed to ~$4x10^{-6}$ Torr. To complete the MIS devices, ~500 nm-thick Al was deposited on MoO_x through a shadow mask having circular openings with a diameter of ~1 mm each. Room temperature I-V measurements were performed using a Potentiostat (Model: Reference 600 Potentiostat/ Galvanostat/ ZRA, M/s Gamry Instruments, Inc., USA).

3. Results and Discussion

3.1. Structural analysis

The thickness of the deposited MoO_x thin films on silicon substrate was determined through the fitting of spectroscopic ellipsometry data. With increase in DC power from 20 W to 100 W, the thickness and deposition rate increased from 61 nm (3.06 nm/min) to 367 nm (18.6 nm/min) as shown in Figure. 1 (a). The DC power is varied by incremental variation of dc current and as per the sputtering physics, the current determines the number of ions bombarding the target surface

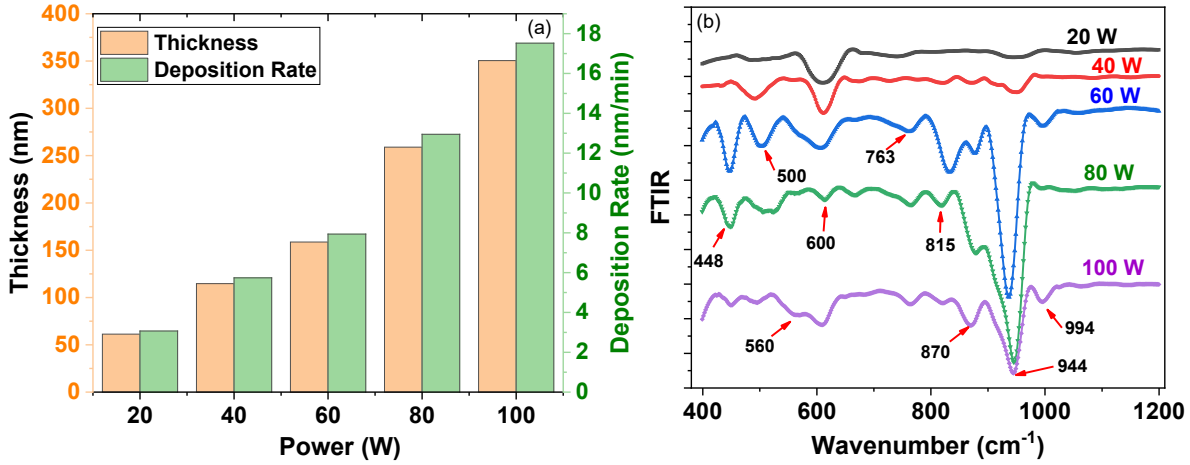

Figure 1. (a). Thickness of MoO_x layer as determined by the fitting of spectroscopic ellipsometry data. (b) FTIR spectra of the as-deposited MoO_x thin films on Si surface with varying DC power.

[14]. It is thus directly proportional to the sputtering rate. The increase in the energy and hence the density of ionized ions, leads to increase in deposition rate. FTIR spectroscopy was used to understand the changes in bonding configuration of MoO_x with varying dc power as shown in Figure 1(b). The stretching vibrations of O atoms in the O-Mo-O units were attributed to the vibration bands around 450 cm^{-1} and 500 cm^{-1} [15]. The bands at around 578 cm^{-1} and 610 cm^{-1} were assigned to the bending vibrations of Mo-O-Mo units [15,16]. Vibration around 562 cm^{-1} is assigned to the extending method of triply composed oxygen came about because of the edge-imparted oxygen in like manner to three MoO_6 octahedral [16,17], which becomes more extensive after decrease. The absence of sharp peaks at low dc power is attributed to the wide range of bond angles and bond lengths present in amorphous films. Peak at 994 cm^{-1} is due to terminal Mo=O bond, which is an indicator of layered orthorhombic MoO_3 phase [17]. Absorption at 808 cm^{-1} is due to stretching mode vibration of bridging oxygen in Mo-O-Mo [17]. The stretching vibrational mode of Mo=O is observed in the range of 840 cm^{-1} to 1000 cm^{-1}, where the peaks are related to Mo-O $(3,3^1)$-Mo at 877 cm^{-1} and Mo-O (2^1)-Mo at 819 cm^{-1} as explained by Rao et al., [18] with the schematic model of oxygen coordination with the Mo atom.

3.2. **Optical analysis**

The optical transmittance spectra of the as-deposited MoO_x films with varying DC power are shown in Fig. 2. All the as-deposited films exhibited high-transmittance, > 80% from visible to NIR region. Enhancing the dc current and hence the power increases the energy of the atoms during deposition that improves the crystallinity of the samples and also modulates the oxidation states of atoms. This leads to modulation in the transmittance at higher dc power in spite of higher thickness. The optical band gap of the as-deposited film on glass was estimated from the transmittance spectrum using Tauc's relation:

$$(\alpha h\nu)^2 = A(h\nu - E_G) \quad (1)$$

Here α, $h\nu$ and A are the absorption coefficient, photon energy and a constant. The E_G values were determined by extrapolating the linear portion of the curve on $h\nu$ axis as shown in the inset of Figure 2. The deposited films show decrease in the optical band gap with increase in the dc power. This

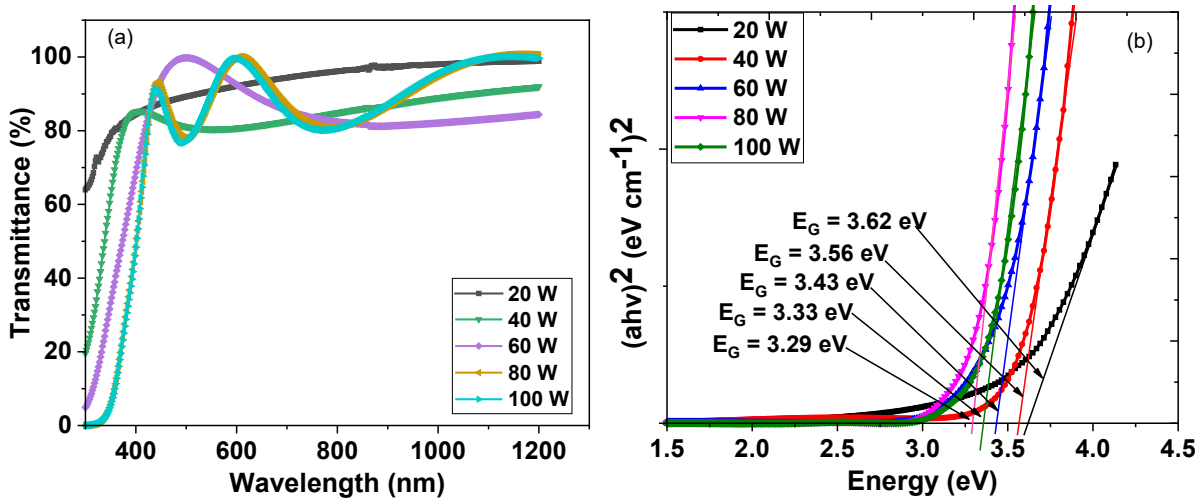

Figure 2. (a). Optical transmittance of the deposited MoO_x layer on glass substrate. (b) Tauc's plot and the calculated bandgap of the as-deposited MoO_x with varying dc power.

is due to the creation of oxygen ion vacancies, which act as positively charged structural defects that are able to capture one or two electrons. The oxygen vacancies occupied by electrons act as donor centers, which lie close to valence band, are responsible for broad band absorption [19, 20].

3.3. Electrical analysis

The quality of MoO_x/n-Si interface with variation in the sputtering power in the range, 20-100 W, was studied using analysis of current-voltage (I-V) measurements as shown in Figure 3.

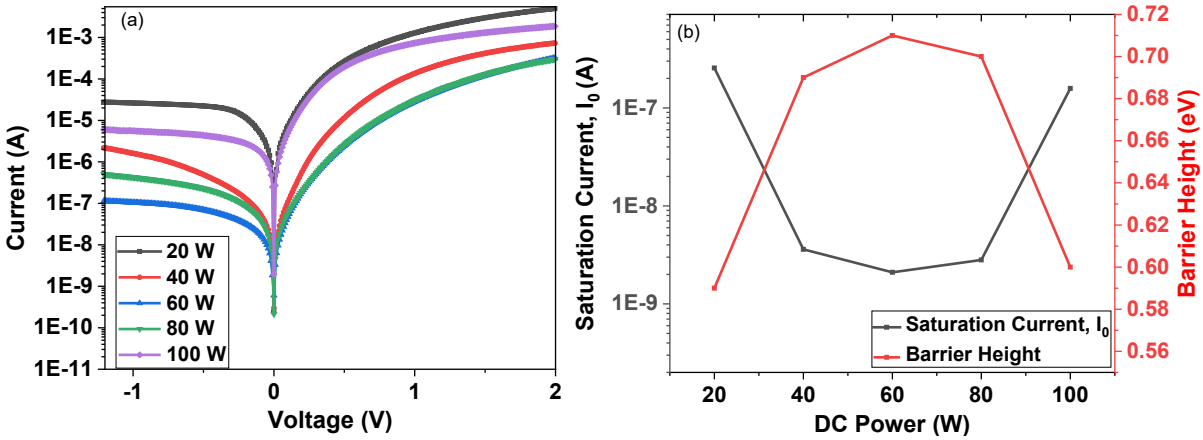

Figure 3. (a). I-V characteristics of the as-deposited MoO_x layer on n-Si substrate. (b) Barrier Height and Reverse saturation current as extracted from I-V characteristics for different samples.

The device has a good rectifying property, as evidenced by its weak reverse current dependence on reverse bias in addition to its significant forward current dependence on forward bias. From the I-V curves, the influence of dc power variation is clearly seen. There is decrease in the reverse leakage current with increasing the power from 20 W to 60 W and then a significant increase at higher power of 80 W and 100 W. The barrier height ϕ_b and the reverse leakage current I_0 are calculated from the I-V characteristics by conventional method and the variation with power is shown in Figure 3.

Taking the derivative of forward and reverse currents with respect to the applied voltage, the device's junction resistance (R_J) was calculated from the I–V data, (R_J = dV/dI) [21]. The plot of R_J versus applied voltage is depicted in Fig. 4. Accordingly, the values of series

resistance (R_s) and shunt resistance (R_{sh}) were determined. The electrode resistances, the bulk Si semiconductor substrate, and the MoO_x layer all give rise to R_s. R_{sh} is caused by contact currents of varying polarities and leakage current at the device's depletion region and both device edges [21]. Figure 4, shows the variation of R_s and R_{sh} of MoO_x/Si structure with variation of DC power. The value of R_{sh} increases with increase in power up to 60 W, which due to improvement in the crystal structure leading to less leakage current, while increase is R_s is basically due to increase in the resistance offered by MoO_x layer with increase in thickness. While at higher power the presence of elemental Mo along with MoO_x and non-uniform distribution of structure provides path for currents hence R_{sh} and R_s decrease at higher dc power.

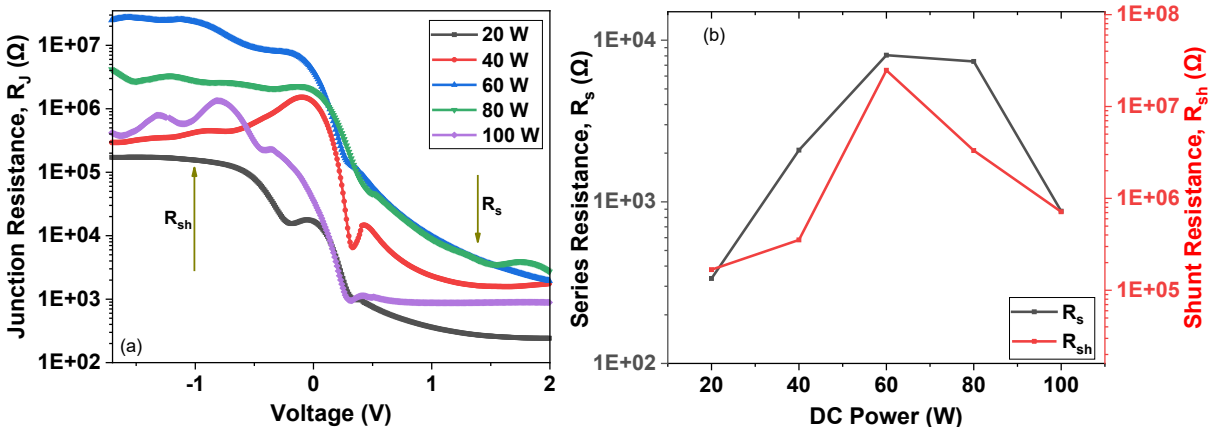

Figure 4. (a). Junction resistance, R_J calculated from the I-V characteristics of the as-deposited MoO_x layer on n-Si substrate. (b) Shunt resistance, R_{sh} and series resistance, R_s obtained from the junction resistance.

Table 1. Parameters extracted from the current-voltage characteristics of MoO_x/n-Si interface.

Power (W)	**Φ_b (eV)**	**I_o (A)**	**R_s (Ω)**	**R_{sh} (kΩ)**
20	0.59	2.55×10^{-7}	335	167.80
40	0.69	3.60×10^{-9}	2088	353.45
60	0.71	2.10×10^{-9}	8072	24775.1
80	0.70	2.81×10^{-9}	7389	3315.187
100	0.60	1.58×10^{-7}	874	714.321

The parameters extracted from the electrical measurements have been summarized in Table 1.

4. Conclusion

The tuning of optical properties of MoO_x and electronic properties of MoO_x/n-Si interface with variation in sputtering power has been presented in detail for its applicability as carrier selective contacts in photovoltaic devices. The films showed higher optical transmittance (> 80%) in the visible and near infrared region of the spectrum and further improved with sputtering power.

The decrease in optical band gap from 3.70 eV to 3.23 eV with DC power was observed due to the creation of oxygen ion vacancies. The low value of optical band gap of 3.23 eV at the higher sputtering power was due to the presence of MoO_x along with the elemental molybdenum. The electrical properties of MoO_x/n-Si interface analyzed using I-V measurements showed a significant change in the selectivity parameters, like barrier height ϕ_b, I_0 and series resistance of MoO_x with dc power. The barrier height ϕ_b decreases at lower and higher dc power and remains almost same (0.69 eV to 0.71 eV). Opposite behavior for leakage current I_0 has been observed with a minimum at 60 W. These extracted parameters showed that the sputtering power has a great influence on the selectivity of the charge carriers. So, we can conclude that intermediate power of 40 W shows higher band gap, higher barrier height and low leakage current with lower series resistance, hence favorable for making selective contacts in silicon solar cells.

Credit authorship contribution statement

Abhishek Kumar: Writing- original draft, Investigation, Data curation, Conceptualization. **Jyoti**: Review & Editing, Data Curation. **Shweta Tomer**: Review & Editing, Data Curation. **Vandana:** Review & Editing, Supervision. **Sanjay Kumar Srivastava**: Review & Editing. **Mrinal Dutta**: Review & Editing. **Prathap Pathi**: Review & Editing, Data curation, Supervision, Resources.

Data availability

The raw/processed data can be supplied on specific requests to the authors.

Declaration of competing interest

The authors declare that they have no known competing financial interests or personal relationships that could have appeared to influence the work reported in this paper.

Acknowledgement

The authors are thankful to CSIR-National Physical Laboratory, New Delhi for providing the experimental facilities. The author Abhishek Kumar gratefully acknowledges the support of Ministry of New and Renewable Energy (MNRE), Govt. of India for providing NREF fellowship.

References

1. L. G. Gerling, S. Mahato, A. M. Vilches, G. Masmitja, P. Ortega, C. Voz, R. Alcubilla, J. Puigdollers, “Transition metal oxides as hole-selective contacts in silicon heterojunctions solar cells,” *Sol. Energy Mater. Sol. Cells*, vol. 145, 109, 2016. Doi: 10.1016/j.solmat.2015.08.028.
2. M. Bivour, J. Temmler, H. Steinkemper, and M. Hermle, “Molybdenum and tungsten oxide: High work function wide band gap contact materials for hole selective contacts of silicon solar cells,” *Sol. Energy Mater. Sol. Cells*, vol. 142, 34, 2015. Doi: 10.1016/j.solmat.2015.05.031.
3. T. Xie, G. Liu, B. Wen, J. Y. Ha, N. V. Nguyen, A. Motayed, and R. Debnath, “Tunable ultraviolet photo response in solution-processed p-n junction photodiodes based on transition-metal oxides,” *ACS Appl. Mater. Interfaces*, vol. 7, 9660, 2015. Doi: 10.1021/acsami.5b01420.
4. J. Meyer, S. Hamwi, M. Kröger, W. Kowalsky, T. Riedl, and A. Kahn, “Transition metal oxides for organic electronics: Energetics, device physics and applications,” *Adv. Mater.*, vol. 24, 5408, 2012. Doi: 10.1002/adma.201201630.

5. Z. Hussain, “Optical and electrochromic properties of heated and annealed MoO_3 thin films,” *J. Mater. Res.*, vol. 16, 2695, 2001. Doi: 10.1557/JMR.2001.0369.
6. C. S. Hsu, C. C. Chan, H. T. Huang, C. H. Peng, and W. C. Hsu, “Electrochromic properties of nanocrystalline MoO_3 thin films,” *Thin Solid Films*, vol. 516, 4839, 2008. Doi: 10.1016/j.tsf.2007.09.019.
7. Bobeico E, Mercaldo LV, Morvillo P, Usatii I, Della Noce M, Lancellotti L, Sasso C, Ricciardi R, Delli Veneri P., “Evaporated MoO_x as general back-side hole collector for solar cells,” *Coatings*, vol. 10, 1, 2020. Doi: 10.3390/COATINGS10080763.
8. S. Subbarayudu, V. Madhavi, and S. Uthanna, “Growth of MoO_3 Films by RF Magnetron Sputtering: Studies on the Structural, Optical, and Electrochromic Properties,” vol. 2013, 2013. Doi: https://doi.org/10.1155/2013/806374.
9. R. Yordanov, S. Boyadjiev, V. Georgieva, and L. Vergov, “Characterization of thin MoO_3 films formed by RF and DC-magnetron reactive sputtering for gas sensor applications,” *J. Phys. Conf. Ser.*, vol. 514, no. 1, 2014, Doi: 10.1088/1742-6596/514/1/012040.
10. A. Tyagi, J. Biswas, K. Ghosh, A. Kottantharayil, and S. Lodha, “Performance Analysis of Silicon Carrier Selective Contact Solar Cells with ALD MoO_x as Hole Selective Layer,” *Silicon*, 2021. Doi: 10.1007/s12633-021-00984-x.
11. R. S. Patil, M. D. Uplane, and P. S. Patil, “Structural and optical properties of electrodeposited molybdenum oxide thin films,” *Appl. Surf. Sci.*, vol. 252, 8050, 2006. Doi: 10.1016/j.apsusc.2005.10.016.
12. H. Simchi, B. E. McCandless, T. Meng, J. H. Boyle, and W. N. Shafarman, “Characterization of reactively sputtered molybdenum oxide films for solar cell application,” *J. Appl. Phys.*, vol. 114, 2013. Doi: 10.1063/1.4812587.
13. G. Wang, C. Zhang, H. Sun, Z. Huang, and S. Zhong, “Understanding and design of efficient carrier-selective contacts for solar cells,” vol. 115026, no. July, 2021. Doi: 10.1063/5.0063915.
14. S. Swann, “Magnetron sputtering,” *Phys. Technol.*, vol. 19, 67, 1988. Doi: 10.1088/0305-4624/19/2/304.
15. S. Kumari, K. Singh, P. Singh, S. Kumar, and A. Thakur, “Thickness dependent structural, morphological and optical properties of molybdenum oxide thin films,” *SN Appl. Sci.*, vol. 2, 1, 2020. Doi: 10.1007/s42452-020-3193-2.
16. V. Nirupama and S. Uthanna, “Influence of sputtering power on the physical properties of magnetron sputtered molybdenum oxide films,” *J. Mater. Sci. Mater. Electron.*, vol. 21, 45, 2010. doi: 10.1007/s10854-009-9867-6.
17. Q. Huang, S. Hu, J. Zhuang, and X. Wang, “MoO_{3-x} based hybrids with tunable localized surface plasmon resonances: Chemical oxidation driving transformation from ultrathin nanosheets to nanotubes,” *Chem. - A Eur. J.*, vol. 18, 15283, 2012. Doi: 10.1002/chem.201202630.
18. K. Srinivasa Rao, B. Rajini Kanth, and P. K. Mukhopadhyay, “Optical and IR studies on RF magnetron sputtered ultra-thin MoO_3 films,” *Appl. Phys. A Mater. Sci. Process.*, vol. 96, 985, 2009. Doi: 10.1007/s00339-009-5132-3.
19. M. Mohammadbeigi, L. Jamilpanah, B. Rahmati, S. M. Mohseni, “Sulfurization of planar MoO_3 optical crystals: Enhanced Raman response and surface porosity,” *Mater. Res. Bull.* 118, 110527 (2019). Doi: 10.1016/j.materresbull.2019.110527.
20. M. Rabizadeh, M. H. Ehsani, and M. M. Shahidi, “Tuning of physical properties in MoO_3 thin films deposited by DC sputtering,” *Opt. Quantum Electron.*, vol. 53, 1, 2021. Doi: 10.1007/s11082-021-03360-6.
21. M. M. Makhlouf, H. Khallaf, and M. M. Shehata, “Impedance spectroscopy and transport mechanism of molybdenum oxide thin films for silicon heterojunction solar cell application,” *Appl. Phys. A Mater. Sci. Process.*, vol. 128, 1, 2022. Doi: 10.1007/s00339-021-05215-z.